

Article

A Wide-Angle Scanning Leaky-Wave Antenna Based on a Composite Right/Left-Handed Transmission Line

Shaoyi Xie ^{1,*}, Jiawei Li ¹, Guangjian Deng ¹, Jiaxin Feng ² and Shaoqiu Xiao ²

¹ Northwest Institute of Nuclear Technology, Xi'an 710024, China; lijawei@nint.ac.cn (J.L.); dengguangjian@nint.ac.cn (G.D.)

² School of Physics, University of Electronic Science and Technology of China, Chengdu 610054, China; fengjiaxin059@163.com (J.F.); xiaoshaoqiu@uestc.edu.cn (S.X.)

* Correspondence: xieshaoyi@nint.ac.cn

Received: 12 February 2020; Accepted: 6 March 2020; Published: 11 March 2020



Abstract: This paper presents a frequency-independent, wide-angle scanning leaky-wave antenna (LWA), based on the composite right/left-handed transmission line (CRLH TL). The proposed LWA consists of a coplanar waveguide-grounded (CPWG) structure loaded by varactors. Loaded varactors are used to control the phase constant of the fundamental mode of the LWA by adjusting the applied DC voltage. The LWA has an excellent wide-angle scanning capability, a simple structure, and low cost. Results show that the main beam of an LWA with 20 unit cells can scan from -66° to 62° at the operation frequency of 3.0 GHz, with a peak gain of 9.9 dBi, and a gain fluctuation of less than 4.9 dB. The operation bandwidth and radiation efficiency are about 13% and over 50%, respectively. A 10-unit cascaded LWA prototype was designed, fabricated, and measured to verify the design concept.

Keywords: composite right/left-handed transmission line (CRLH TL); coplanar waveguide ground (CPWG); leaky-wave antenna (LWA); frequency-independent; wide-angle scanning

1. Introduction

Beam-steering antennas are usually adopted for improving the performance of wireless communication and radar systems. The phased array is considered to be one of the most popular choices to steer radiation beams. However, the use of phase shifters in a phased array is associated with high cost and bulkiness. The leaky-wave antenna (LWA) overcomes the shortcomings of the phased array due to its significant advantages, such as simple structure, beam-steering capability, and low cost [1–3]. However, the traditional LWA can only achieve forward or backward beam-scanning. Due to the inherent stop-band of the antenna structure, it is difficult to achieve broadside radiation for the traditional LWA. Moreover, because the traditional LWA operates at higher modes, complex feed structures are needed to suppress the fundamental mode [2].

Metamaterials, which have unique properties, bring new opportunities to the traditional antenna technologies [4–6]. The early proposed metamaterials were lossy and narrow-banded, which limited their applications. The composite right/left-handed transmission line (CRLH TL) has low loss and wide bandwidth. There are plenty of studies on the CRLH TL antenna designs, such as the zeroth-order resonator antenna and LWAs [7,8]. The CRLH TL LWA proposed in [9–13] operates in the fundamental mode and it can achieve continuous backward to forward beam-scanning as the frequency changes. However, the frequency-dependent CRLH TL LWA is not suitable for communication and radar systems that work at a fixed frequency. Researchers proposed frequency-independent CRLH TL LWAs for this purpose. Electronically controlled beam-steering CRLH TL LWAs, working at a fixed frequency, were tested by loading varactors, switches, liquid crystals, and ferrite [14–23]. These studies indicate that the CRLH TL LWAs can greatly improve the performance of the traditional LWAs and have great

application potential in beam-scanning. However, none of them can scan more than $\pm 50^\circ$ [19–23], which is too low for many applications. Consequently, improving the beam-scanning range at a fixed frequency is a significant challenge for current metamaterial-based LWA research.

This paper proposes a frequency-independent, wide-angle scanning LWA based on a CRLH TL, which achieves a beam-scanning range of over $\pm 60^\circ$ at the operating frequency of 3.0 GHz. Moreover, the radiation structure and its DC bias network are very simple. The proposed LWA consists of a coplanar waveguide-grounded (CPWG) structure, periodically varactor-loaded. By establishing an equivalent circuit model, the dispersion curve can be extracted and used to predict the antenna's performance. A 20-unit cascaded LWA was designed; simulation results showed that its main beam can scan from -66° to 62° by changing the loaded varactors' DC bias voltage.

2. Operation Principle and Scheme of the Proposed LWA

2.1. Operation Principle

The Floquet theorem indicates that infinite harmonic components are introduced into LWAs with a periodic structure, and the phase constant of each harmonic component can be expressed as:

$$\beta_n = \beta_0 + \frac{2\pi n}{p} \quad (1)$$

where n is the order of the space harmonic, p is the per-unit length, and β_0 is the phase constant of the fundamental mode. According to the operation principle of the periodic LWA, the radiation condition can be satisfied when the fast wave component is supported in the periodic structure. The LWA based on the CRLH TL has a quasi-uniform periodic structure and it can operate in the fundamental mode and radiate electromagnetic waves. The main beam angle from the broadside can be determined by the phase constant of the fundamental mode and is written as:

$$\theta_0 = \sin^{-1}(\beta_0/k_0) \quad (2)$$

where k_0 is the wave number in free space.

In the frequency-dependent CRLH TL LWA, the backward to forward beam-scanning capability is achieved by varying the frequency. Similarly, the phase constant can also be changed by loading electronically controlled components, such as varactors. As a result, it can be deduced that the beam scanning capability can be achieved at a fixed frequency by controlling the DC bias voltage V of the varactors, which is equivalent to changing the propagation constant of the fundamental mode. Then, the main beam angle can be calculated by:

$$\theta_0 = \sin^{-1}(\beta_0(V)/k_0). \quad (3)$$

2.2. Proposed LWA Configuration

Figure 1a shows the scheme of the proposed LWA, which is a varactor-loaded CPWG structure. The CPWG is composed of a central conductor strip and bilateral strips, which are connected to the ground by metalized vias. The CPWG can restrain back radiation and avoid surface wave leakage. The top view of each unit cell is displayed in Figure 1b. A symmetrical topology is used to equalize the impedance of two ports. Two series varactors with opposite polarity are loaded at the center strip of each unit cell. One end of each varactor is connected to the grounded strip, which is used to apply a negative DC bias voltage. The other end of each varactor is connected to the central conductor strip, which is used to apply a positive DC bias voltage. The barrier capacitance of the varactor varies with the reverse voltage. As the reverse voltage increases, the capacitance decreases. Skyworks SMV2020-079L varactors were used in this study. Based on their manual specifications, these varactors have a variable capacitance range of 0.35 pF–3.20 pF. The applied DC bias voltage varied from 20 V to

0 V. As shown in Figure 1a, 100 nH chip inductors were loaded between the central conductor strip and the positive bias voltage line to isolate the AC signal. On the two ends of the LWA, there are two pF chip capacitors with 0603 packages that isolate the DC signal. Thus, for an LWA with N unit cells, a total of $2N$ varactors, $N + 1$ chip inductors, and two chip capacitors are employed. The antenna structure is supported on the substrate of F4B-2 ($\epsilon_r = 2.65$), with a thickness of 3 mm. Table 1 shows the dimensions of the unit cell structure. The radiation structure and the DC bias network of the varactors are very simple; all varactors can easily acquire the same voltage simultaneously.

To predict the performance of the proposed LWA and better guide future work, an equivalent circuit model of each unit cell was established and is shown in Figure 2. The varactors and the metalized vias serve as left-handed capacitors $C_{L,VAR}$ and left-handed inductors L_L , respectively, while the TL itself provides the right-handed capacitance C_R and the right-handed inductance L_R . Based on this equivalent circuit model, the phase constant of the fundamental mode in the CRLH TL can be derived as:

$$\beta = \frac{1}{p} \cos^{-1} \left(1 + \frac{ZY}{2} \right) \tag{4}$$

$$Z = j \left(\omega L_R - \frac{1}{\omega C_{L,VAR}} \right) \tag{5}$$

$$Y = j \left(\omega C_R - \frac{1}{\omega L_L} \right). \tag{6}$$

The Bloch impedance can be extracted from the S -parameters of the unit cell by (7):

$$Z_B = \frac{2jZ_0 S_{21} \sin(\beta p)}{(1 - S_{11})(1 - S_{22}) - S_{21} S_{12}}. \tag{7}$$

Using Equations (4)–(6), the dispersion curves of the CRLH TL can be obtained, and the Z_B in Equation (7) can be used to optimize the impedance of the unit cell in the LWA.

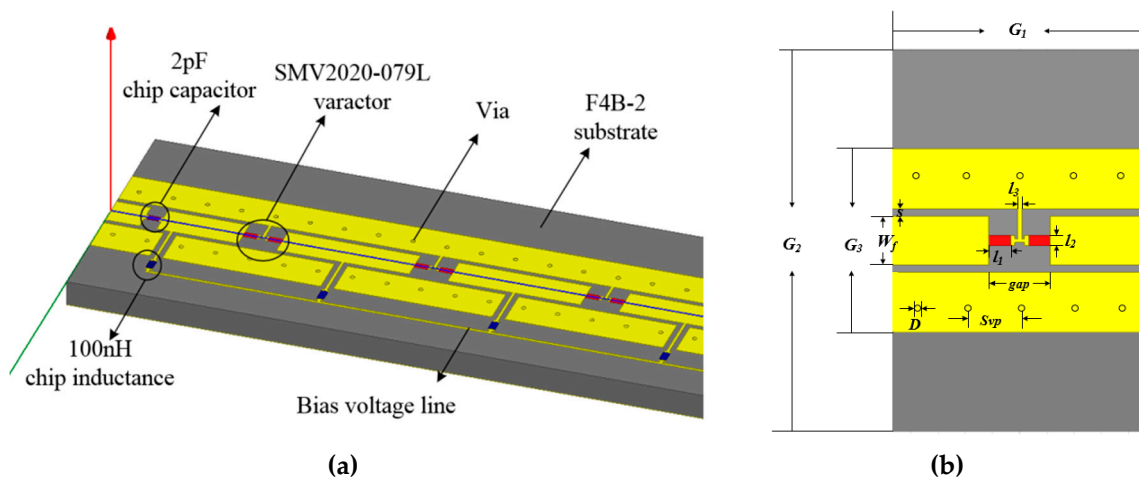


Figure 1. Scheme of the proposed leaky-wave antenna (LWA). (a) Structure of the LWA; (b) Top view of the unit cell.

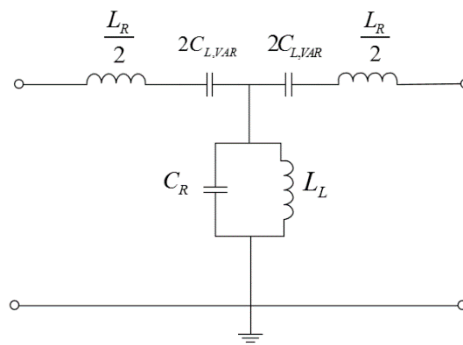


Figure 2. Equivalent circuit model of the unit cell.

Table 1. Dimensions of the unit cell(unit:mm).

G ₁	G ₂	G ₃	W _f	S	S _{vp}
20	31	15	4	0.6	4
D	gap	l ₁	l ₂	l ₃	
0.5	4.5	1.6	0.8	0.3	

3. LWA Design and Experiment Results

3.1. Simulated Results for the Unit Cell

The electromagnetic full-wave analysis software Ansoft HFSS was used to simulate the proposed LWA. Firstly, the S_{11} of the unit cell with various series capacitances was simulated; the simulation’s results indicate that the amplitude of S_{11} ($|S_{11}|$) in dB is less than -10 dB when the capacitance varies from 0.38 pF to 1.9 pF at the frequency of 3.0 – 4.0 GHz. In practice, the capacitance variation is controlled by the loaded varactors with different DC bias voltages. Figure 3 shows the simulated $|S_{11}|$ in dB when the capacitance $C_{L,var}$ equals several selected values, i.e., 0.6 pF, 1.0 pF, and 1.9 pF. The $|S_{11}|$ that corresponds to these capacitances at 3.2 GHz is -21.5 dB, -20.7 dB, and -14.8 dB, respectively.

The parameters of the equivalent circuit model in Figure 2 can be extracted from the S-parameters of the unit cell through the parametric fitting method. The extracted results are shown in Table 2. The dispersion diagram of the TL structure, which consists of infinite unit cells, was extracted based on Equations (4)–(6) and is shown in Figure 4. It can be deduced from Figure 4 that, with the increase of the capacitance values of the varactors, the dispersion curves are shifted down in a vertical direction. Based on this phenomenon, the scanning properties of the proposed LWA with a large number of unit cells can be predicted. At the frequency of 3.2 GHz, positive, zero, and negative phase constants can be obtained with different varactor capacitance values. As a consequence, the continuous backward to forward beam-scanning can be achieved at 3.2 GHz.

The Bloch impedance Z_B was calculated using Equation (7). The Bloch impedance Z_B with $C_{L,var} = 1.3$ pF is shown in Figure 5 as an example. Figure 5 shows that the real part of the extracted Bloch impedance is about 50Ω , from 2.8 GHz to 5.5 GHz, and the real part tends to zero. According to other simulation results, the Bloch impedance of around 50Ω can also be obtained with other loaded capacitances in a wide bandwidth.

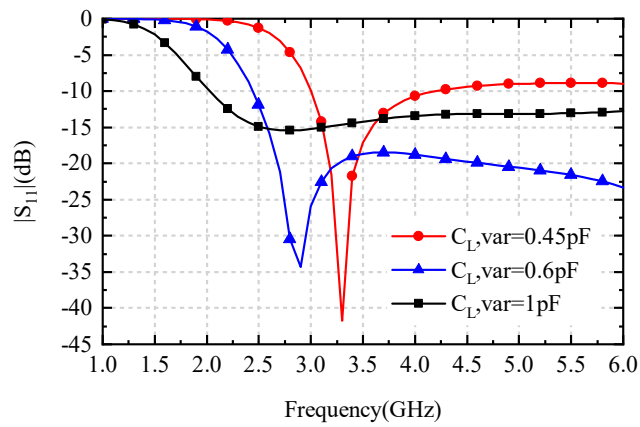


Figure 3. $|S_{11}|$ of the unit with different capacitance values.

Table 2. Extracted equivalent circuit model parameters at 3.2 GHz.

	5 V	10 V	15 V	20 V
$C_{L,var}$ (pF)	1.19	0.57	0.41	0.35
L_L (nH)	1.82	1.53	1.01	0.77
C_R (pF)			1.95	
L_R (nH)			9.78	

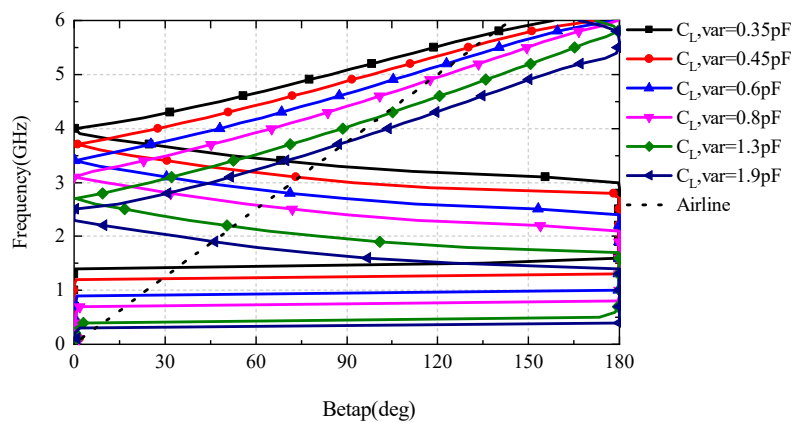


Figure 4. Dispersion diagram of the unit cell with various capacitances of varactors.

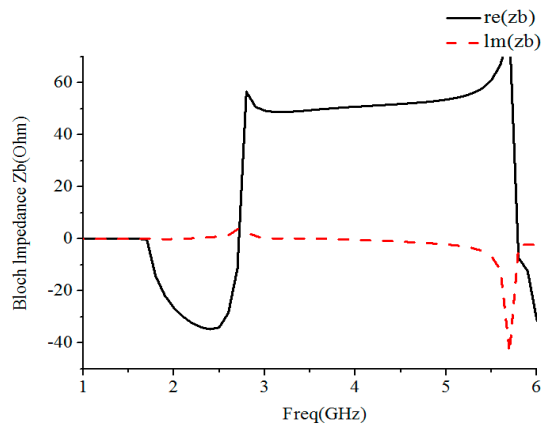


Figure 5. Extracted Bloch impedance of the unit cell with $C_{L,var} = 1.3$ pF.

3.2. Simulated Results of the LWA with Finite Unit Cells

An LWA with 20 cascaded unit cells has a length of about 4λ (λ is the operation wavelength in free space). The scanning performance of the main beam can be predicted using the study described in Section 2.1. However, there are some deviations between the characteristics of the actual LWA and the infinite periodic TL from Section 2.1, in which the mutual coupling effects are ignored among the unit cells. The S_{11} and S_{21} of the designed LWA were calculated when the $C_{L,var}$ changed from 0.35 pF to 1.9 pF. Figure 6 shows the simulated $|S_{11}|$ and $|S_{21}|$ in dB with $C_{L,var} = 0.45$ pF, 0.6 pF, and 1.0 pF, respectively. Figure 6 and the results with other loaded capacitances show that the designed 20-unit cell LWA can be matched well at 3.0 GHz; the fractional bandwidth is 13% with $|S_{11}|$ less than -7.5 dB. The slight shift in the frequency comes from the mutual coupling among the unit cells. Besides this, high radiation efficiency was also obtained; the lowest radiation efficiency was about 50% when the $C_{L,var}$ changed. The efficiency can be improved by increasing the number of unit cells in the LWA. According to the authors' calculation, the LWA could reach a high radiation efficiency of over 80% when the length of the LWA is extended to more than 80 unit cells.

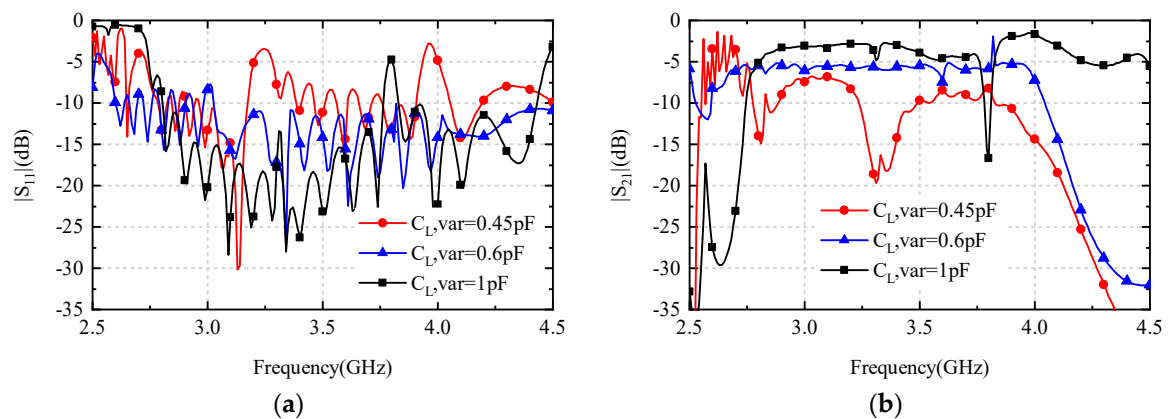


Figure 6. $|S_{11}|$ and $|S_{21}|$ of a 20-cell LWA with different capacitance values. (a) $|S_{11}|$; (b) $|S_{21}|$.

The scanning patterns of the LWA at 3.0 GHz are shown in Figure 7. Figure 7 shows that the scanning angles θ_0 of -66° , -33° , -20° , 0° , 8° , 29° , 42° , and 62° were achieved when the $C_{L,var}$ was equal to 0.38 pF, 0.45 pF, 0.5 pF, 0.6 pF, 0.7 pF, 1 pF, 1.3 pF, and 1.9 pF, respectively. As the capacitance increased, the main beams were steered from the back to the fore gradually; a scanning range of 128° (from -66° to 62°) was obtained when the capacitance of the varactors changed from 0.38 pF to 1.9 pF. The cross-polarization components are shown here due to their lower level as compared with the co-polarization radiation. In addition, the side lobe level (SLL) was also low over the entire beam-scanning range because of the gradual distribution of the current amplitude in the LWA aperture.

It should be noted that broadside radiation is achieved when the $C_{L,var} = 0.6$ pF in Figure 7. Generally speaking, an unbalanced condition is easy to generate because of the sensibility to broadside radiation. Consequently, it is a common phenomenon in the periodical LWA that the realized gain decreases significantly at the broadside [5,6]. However, for the proposed LWA, the balance condition is satisfied at $C_{L,var} = 0.6$ pF. Therefore, the stop band and decline of the realized gain do not happen for broadside radiation.

In Figure 7, the peak gain of the scanning beams is 9.9 dBi; the minimum gain of 5.0 dBi appears at scanning angle $\theta_0 = 62^\circ$. Gain fluctuation over the entire scanning range is about 4.9 dBi. The main reason for the lower gain at larger radiation angles off the broadside direction is the decrease in the effective aperture area to the direction of low elevation (equivalent to low leakage efficiency). As mentioned in the discussion of radiation efficiency, the gain can also be improved by increasing the number of unit cells in the LWA.

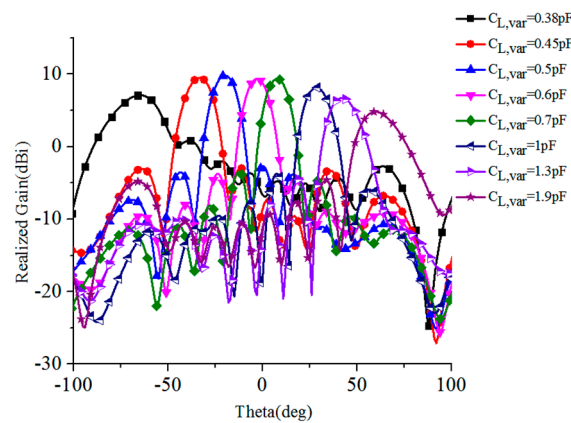


Figure 7. Simulated radiation patterns with capacitance varied from 0.38 pF to 1.9 pF.

Figure 8a shows the scanning angles versus the $C_{L,var}$. As mentioned above, the proposed LWA achieves a beam-steering range of 128° with a small gain fluctuation. This excellent beam-scanning ability in a wide angle range comes from the particular LWA structure and the wide capacitance variation range of the loaded varactors. Figure 8b shows the half-power beam width (HPBW) of the scanning beam in the scanning plane (E-plane) with different loaded capacitance values. When the LWA radiates to a larger angle off the broadside direction, the HPBW becomes wider.

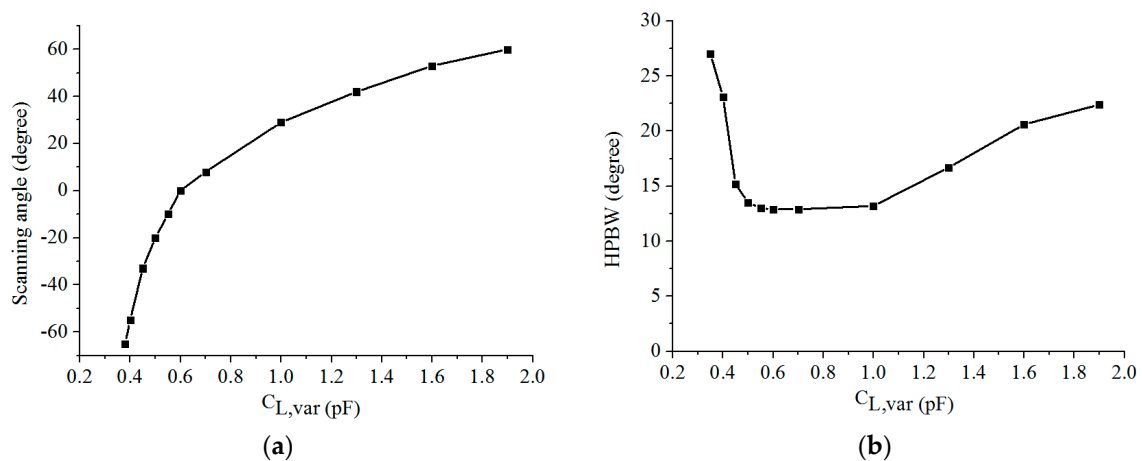


Figure 8. Scanning angle and half-power beamwidth (HPBW) of the LWA versus $C_{L,var}$. (a) Scanning angle; (b) HPBW.

The reason behind this phenomenon is the same as that given in the gain variation analysis mentioned above. Table 3 shows a comparison among the performances of several previous studies [19–21] with the proposed LWA. It shows that the proposed LWA achieves the largest beam-scanning range.

Table 3. Comparison of electronically controlled composite right/left-handed (CRLH) LWAs.

Ref.	Simulated Scanning Range	Measured Scanning Range	Overall Length	Realized Gain (dBi)
[21]	-38° – $+30^\circ$	-17° – $+40^\circ$	3.25λ	3.1–6.2
[20]	-38.6° – $+53.3^\circ$	-31° – $+35^\circ$	3.25λ	7.8–11.3
[19]	-49° – $+50^\circ$	-35° – $+38^\circ$	5.87λ	–7.0–18.0
This work	-66° – $+62^\circ$	-60° – $+60^\circ$	4λ	5–9.9 ¹

¹ The simulated realized gain was adopted because only a prototype with a length of 2λ was measured in this work.

3.3. Fabrication and Measurement

The LWA was fabricated and measured to verify the design concept. Since a substrate with a length of 4λ (40 cm) and its etching process are not available in our laboratory, a prototype of a 10-unit cascaded LWA was fabricated to demonstrate the performance of the proposed LWA, which is shown in Figure 9a,b. The measured $|S_{11}|$ and $|S_{21}|$ in dB with three different bias voltages of the varactors are shown in Figure 10; those with other DC bias voltages are omitted in this figure for brevity. The measured results indicate that the LWA can be matched well at around 3.0 GHz, which is similar to the designed results of the 20-unit cascaded LWA (see Figure 6).

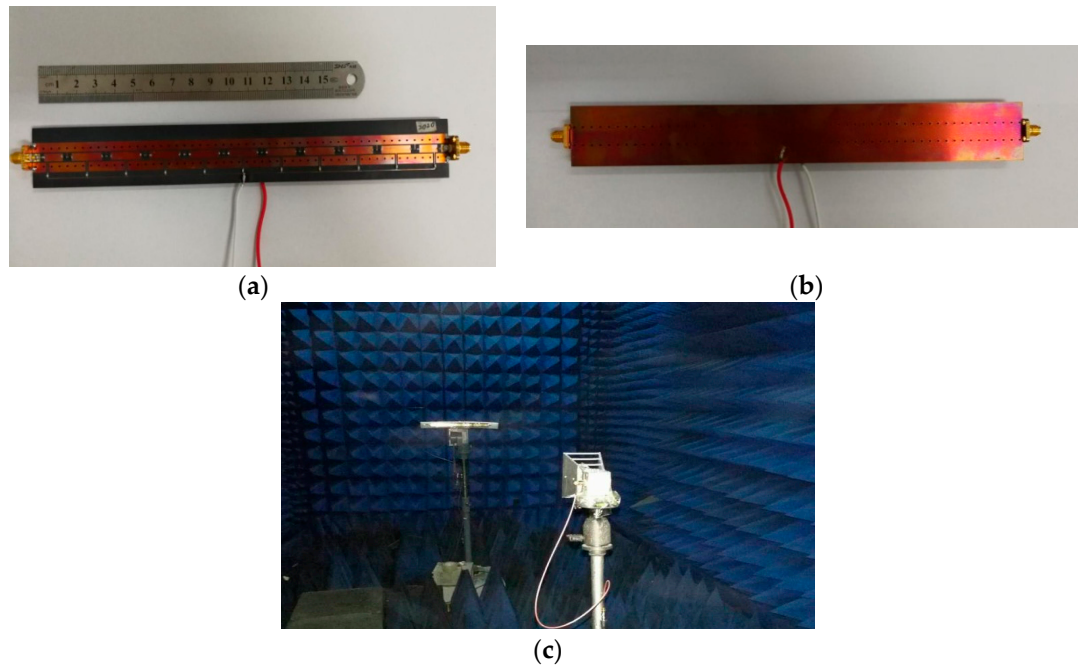


Figure 9. Photograph of the fabricated 10-unit LWA prototype. (a) Top view; (b) Bottom view; (c) Measurement installation.

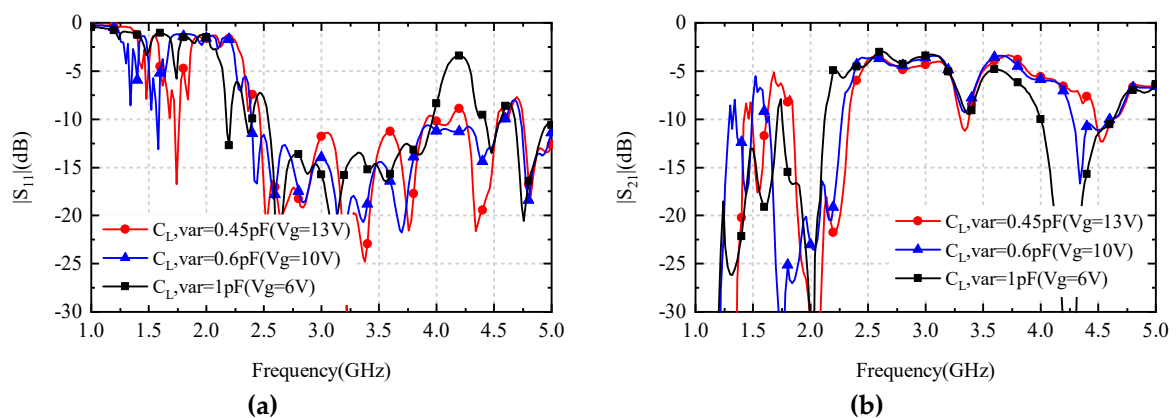


Figure 10. Measured S-parameters of the overall antenna. (a) S_{11} ; (b) S_{21} .

Figure 9c shows the measurement installation of the far field radiation pattern in the anechoic chamber. Figure 11 shows the measured normalized radiation patterns in co-polarization under different DC bias voltages of the loaded varactors. A scanning range from -60° to 60° was observed when the applied voltage varied from 17 V to 2 V. Similarly, low SLL characteristics were still observed, as shown in the simulations in Figure 7. By comparing Figure 11 with Figure 7, it can be seen that

the measured scanning range of the main beam matches that of the designed 20-unit cascaded LWA. On the whole, the simple radiation structure and DC feed network for the varactors result in only a small deviation between the experimental results and the proposed LWA's results. This slight deviation between simulation and measurement is due to the fabrication tolerances and the used varactor model.

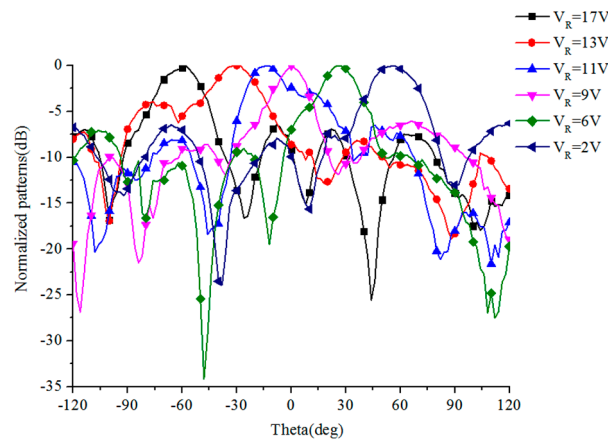


Figure 11. Measured normalized radiation patterns under different bias voltages.

The measured beam-scanning range of the proposed LWA is listed in Table 3, which is compared with the three previous LWAs proposed in [19–21]. Just as with the simulated results, the proposed LWA possesses the widest beam-scanning range. This study demonstrates that the proposed LWA has broad application prospects in wide angle scanning applications.

4. Conclusions

This paper proposes a frequency-independent wide-angle scanning LWA based on a CRLH TL. It operates at a frequency of 3.0 GHz with a fractional bandwidth of 13%. ACPWG structure is used for the frequency-independent LWA. The phase constant of the fundamental mode in the LWA is controlled by changing the applied DC voltage of the periodically loaded varactors. A scanning range of 128° (from -66° to 62°) is achieved with a low SLL and a low gain fluctuation by the designed 20-unit cell LWA. The peak gain is 9.9 dBi and the lowest radiation efficiency is about 50% during beam-scanning. The experimental verification is completed by fabricating and measuring a prototype—a 10-unit cascaded LWA.

Author Contributions: Antenna design, investigation and data curation, S.X. (Shaoyi Xie) and J.L.; Formal analysis, J.L.; Funding acquisition and project administration, G.D.; Methodology, simulation and writing, J.F. and S.X. (Shaoqiu Xiao); All authors have read and agreed to the published version of the manuscript.

Funding: This work was supported in part by the National Natural Science Foundation of China under Grant 61731005, and in part by the Pre-research Foundation of National Defense of China under Grant 170441413086.

Conflicts of Interest: The authors declare no conflict of interest.

References

- Oliner, A.A. Leakage from higher modes on microstrip line with application to antennas. *Radio Sci.* **1987**, *22*, 907–912. [[CrossRef](#)]
- Jackson, D.R. Leaky-wave antennas. In *Frontiers in Antennas: Next Generation Design & Engineering*; Caloz, C., Jackson, D.R., Itoh, T., Eds.; McGraw-Hill: New York, NY, USA, 2011; pp. 339–406.
- Liu, J.; Jackson, D.R.; Long, Y. Substrate Integrated Waveguide (SIW) Leaky-Wave Antenna with Transverse Slots. *IEEE Trans. Antennas Propag.* **2011**, *60*, 20–29. [[CrossRef](#)]
- Shelby, R.A.; Smith, D.R.; Schultz, S. Experimental Verification of a Negative Index of Refraction. *Science* **2001**, *292*, 77–79. [[CrossRef](#)] [[PubMed](#)]

5. Caloz, C.; Itoh, T. *Electromagnetic Metamaterials: Transmission Line Theory and Microwave Applications*; Wiley: Hoboken, NJ, USA, 2005; pp. 261–313.
6. Eleftheriades, G.V.; Balmain, K.G. *Negative Fraction Metamaterials: Fundamental Principles and Applications*; Wiley: Hoboken, NJ, USA, 2005; pp. 53–92.
7. Sanada, A.; Kimura, M.; Awai, I.; Kubo, H.; Caloz, C.; Itoh, T. A planar zeroth order resonator antenna using left-handed transmission line. In Proceedings of the 34th European Microwave Conference, Amsterdam, The Netherlands, 12–14 October 2004.
8. Caloz, C.; Sanada, A.; Itoh, T. A novel composite right-/left-handed coupled-line directional coupler with arbitrary coupling level and broad bandwidth. *IEEE Trans. Microw. Theory Tech.* **2004**, *52*, 980–992. [[CrossRef](#)]
9. Dong, Y.; Itoh, T. Substrate integrated composite right-/left-handed leaky-wave structure for polarization-flexible antenna application. *IEEE Trans. Antenna Propag.* **2012**, *60*, 760–771. [[CrossRef](#)]
10. Cao, W.; Chen, Z.N.; Hong, W.; Zhang, B.; Liu, A. A beam scanning leaky-wave slot antenna with enhanced scanning angle range and flat gain characteristic using composite phase-shifting transmission line. *IEEE Trans. Antennas Propag.* **2014**, *62*, 5871–5875. [[CrossRef](#)]
11. Yang, Q.; Zhao, X.; Zhang, Y. Composite right/left-handed ridge substrate integrated waveguide slot array antennas. *IEEE Trans. Antennas Propag.* **2014**, *62*, 2311–2316. [[CrossRef](#)]
12. Nasimuddin; Chen, Z.N.; Qing, X. Multilayered composite right/left-handed leaky-wave antenna with consistent gain. *IEEE Trans. Antennas Propag.* **2012**, *60*, 5056–5062. [[CrossRef](#)]
13. Saghati, A.P.; Mirsalehi, M.M.; Neshati, M.H. A HMSIW circularly polarized leaky-wave antenna with backward, broadside, and forward radiation. *IEEE Antennas Wirel. Propag. Lett.* **2014**, *13*, 451–454. [[CrossRef](#)]
14. Huang, L.; Chiao, J.-C.; De Lisio, M. An electronically switchable leaky wave antenna. *IEEE Trans. Antennas Propag.* **2000**, *48*, 1769–1772. [[CrossRef](#)]
15. Ouedraogo, R.O.; Rothwell, E.; Greetis, B.J. A reconfigurable microstrip leaky-wave antenna with a broadly steerable beam. *IEEE Trans. Antennas Propag.* **2011**, *59*, 3080–3083. [[CrossRef](#)]
16. Karmokar, D.K.; Esselle, K.P.; Hay, S.G. Fixed-Frequency beam steering of microstrip leaky-wave antennas using binary switches. *IEEE Trans. Antennas Propag.* **2016**, *64*, 2146–2154. [[CrossRef](#)]
17. Sajin, G.; Simion, S.; Craciunoiu, F.; Muller, A.; Bunea, A.C. Frequency tuning of a CRLH CPW antenna on ferrite substrate by magnetic biasing field. In Proceedings of the 39th European Microwave Conference, Rome, Italy, 28–29 September 2009; pp. 1283–1286.
18. Che, B.-J.; Jin, T.; Erni, D.; Meng, F.-Y.; Lyu, Y.-L.; Wu, Q. Electrically controllable composite right/left-handed leaky-wave antenna using liquid crystals in PCB technology. *IEEE Trans. Components Packag. Manuf. Technol.* **2017**, *7*, 1331–1342. [[CrossRef](#)]
19. Lim, S.; Caloz, C.; Itoh, T. Metamaterial-based electronically controlled transmission-line structure as a novel leaky-wave antenna with tunable radiation angle and beamwidth. *IEEE Trans. Microw. Theory Tech.* **2005**, *53*, 161–173. [[CrossRef](#)]
20. Suntives, A.; Hum, S.V. A fixed-frequency beam-steerable half-mode substrate integrated waveguide leaky-wave antenna. *IEEE Trans. Antennas Propag.* **2012**, *60*, 2540–2544. [[CrossRef](#)]
21. Fu, J.-H.; Li, A.; Chen, W.; Lv, B.; Wang, Z.; Li, P.; Wu, Q. An electrically controlled CRLH-inspired circularly polarized leaky-wave antenna. *IEEE Antennas Wirel. Propag. Lett.* **2016**, *16*, 760–763. [[CrossRef](#)]
22. Lee, N.; Lee, S.; Cheon, C.; Kwon, Y. A two-dimensional beam scanning antenna array using composite right/left handed microstrip leaky-wave antennas. In Proceedings of the 2007 IEEE/MTT-S International Microwave Symposium, Honolulu, HI, USA, 3–8 June 2007; pp. 1883–1886.
23. Kaneda, T.; Sanada, A.; Kubo, H. Design of an 8-element planar composite right/left-handed leaky wave antenna array for 2-D beam steering. In Proceedings of the 2006 Asia-Pacific Microwave Conference, Yokohama, Japan, 12–15 December 2006; pp. 1067–1070.

